applied sciences

MDPI

Article

Loop Modeling of the Reciprocal Inhibition Between HPA and HPG Endocrine Axes Reveals Transitions to Bistability and Critical Bifurcation Parameters

Ilaria Demori [1], Seth Siriya [2] and Bruno Burlando [1,*]

[1] Department of Pharmacy, DIFAR, University of Genova, Viale Benedetto XV, 3, 16132 Genova, Italy; ilaria.demori@unige.it
[2] Institute of Automatic Control, Leibniz Universität Hannover, Appelstr. 11, 30167 Hannover, Germany; siriya@irt.uni-hannover.de
* Correspondence: bruno.pietro.burlando@unige.it

Featured Application

This study presents a new model of a well-known physiological mechanism: the reciprocal inhibition between the hypothalamic–pituitary–adrenal (HPA) and hypothalamic–pituitary–gonadal (HPG) endocrine axes. The model reveals transitions to bistability which, according to a paradigm proposed by one of us (B.B.), represents an essential step for the insurgence of pathogenesis in physiological systems. In this context, bistability could give rise, for example, to stress-induced, gender-related neuroendocrine disorders. Through bifurcation analysis, the model also identifies critical bifurcation parameters, linking them to their biological counterparts as potential therapeutic targets. In summary, the analysis provides direct insights for the development of new and effective treatments for a range of poorly understood and difficult-to-treat disorders.

Abstract

Endocrine axes are pathways of interactions involved in various aspects of the organism's functioning, also implicated in deviations from physiological states leading to pathological conditions. The hypothalamic–pituitary–adrenal (HPA) axis releases corticosteroid hormones promoting adaptation to environmental stimuli (acute stress) or inducing altered conditions due to long-term noxious solicitations (chronic stress). The HP–gonadal (HPG) axis regulates reproductive activities by releasing gonadal steroids. These axes have been shown to engage in reciprocal inhibition under certain conditions, particularly when they rise beyond normal ultradian and circadian fluctuations. Based on the literature data, we reconstructed a neuroendocrine network responsible for this type of interaction. Thereafter, we developed a model of the HPA-HPG inhibition based on a series of nonlinear interactions represented by a system of differential equations in the Matlab environment. The quantitative analysis of the system's behavior revealed the occurrence of bifurcations leading to bistable behavior, allowing us to detect bifurcation parameters. Bifurcation arises as the system's components increase hypersensitivity and sustained activity in response to activating inputs. This involves transition from a single low-activity attractor to two distinct attractors, with a new high-activity state representing a breakdown of homeostasis. These results provide insights into the potential involvement of the HPA-HPG interaction in neuroendocrine disorders, and the identification of therapeutic targets from bifurcation parameters.

Academic Editor: Jing Jin

Received: 2 September 2025
Revised: 25 September 2025
Accepted: 26 September 2025
Published: 27 September 2025

Citation: Demori, I.; Siriya, S.; Burlando, B. Loop Modeling of the Reciprocal Inhibition Between HPA and HPG Endocrine Axes Reveals Transitions to Bistability and Critical Bifurcation Parameters. *Appl. Sci.* **2025**, *15*, 10483. https://doi.org/10.3390/app151910483

Keywords: hypothalamic–pituitary–adrenal axis; hypothalamic–pituitary–gonadal axis; closed-loop interactions; nonlinear dynamic system; bifurcation analysis; neuroendocrine disorders; therapeutic targets

1. Introduction

The term 'interaction' most accurately captures the essence and objectives of physiology. Biological systems can be understood as emergent phenomena resulting from a network of interactions among elements producing physical changes. In fields such as medicine and biotechnology, controlling and manipulating these systems is crucial for restoring physiological conditions or for engineering and utilizing them effectively. Achieving these goals requires not only identifying the interacting components but also accurately modeling the patterns of their interactions. The rise of systems biology has marked a growing interest in the dynamics of biological systems. This area has been the cradle of the idea that closed loops of interactions are the predominant, or even exclusive, arrangement in these systems, so to be considered a hallmark of life [1–3]. A key element supporting this interpretation is the intricate network of crosstalk between metabolic and signal transduction pathways and their implications for health and disease [4,5].

Endocrine axes have been long established as pathways of interactions involved in various aspects of the organism's functioning, and are therefore also implicated in deviations from physiological states, leading to pathological conditions. The hypothalamic–pituitary–adrenal (HPA) axis has been identified following the discovery of a cascade of interactions starting from the hypothalamus and proceeding with the anterior pituitary and adrenal glands. It leads to the release of corticosteroid hormones promoting adaptation to environmental stimuli (acute stress) or inducing altered conditions due to long-term noxious solicitations (chronic stress) [6]. Similarly, the HP–gonadal (HPG) axis proceeds from the hypothalamus to the anterior pituitary and gonads, leading to the release of gonadal steroids into the plasma [7]. As further confirmation of the generalized crosstalk among pathways, these axes have been shown to engage in reciprocal inhibition under certain conditions, particularly when they rise beyond normal circadian fluctuations [8].

In studies on both cycling and postmenopausal women, based on circadian fluctuations of cortisol and progesterone, the interaction between the two axes has not been detected [9,10]. By contrast, HPA-HPG interactions have been observed when higher hormone fluctuations were induced by physiological or pharmacological agents [11]. For instance, various studies on women have shown an inverse correlation between circadian progesterone and cortisol during pregnancy [3,12], and HPG axis suppression caused by cortisol [13] and hydrocortisone injections [14]. Additionally, circadian increases in allopregnanolone and reductions in cortisol have been observed in premenstrual dysphoric disorder (PMDD) [15]. In males, cortisol injections have been shown to lower plasma testosterone [16], while exercise has induced a rise in cortisol and a decrease in testosterone [17]; moreover, testosterone replacement has been found to reduce the cortisol response to corticotropin-releasing hormone (CRH) [18]. Such a complex of data suggests that there is a reciprocal inhibition between HPA and HPG axes, which becomes measurable and significant when either or both axes increase their activity beyond physiological circadian oscillations.

The neuroendocrine network responsible for this type of interaction can be reconstructed with a certain degree of precision from the literature data, but the dynamics of the system have never been explored. In this study, we develop a model of the HPA-HPG system allowing us to investigate its dynamics, providing insights into the potential involvement in neuroendocrine disorders and identifying possible targets for restoring physiological conditions.

2. Methods

2.1. Literature Survey

A literature search was conducted in PubMed to reconstruct a loop-based interaction system representing reciprocal inhibition between the HPA and HPG axes. Studies published up to July 2025 were identified using the following main keywords in Boolean operators: (hypothalamic[Title/Abstract] AND pituitary[Title/Abstract] AND adrenal[Title/Abstract] AND axis[Title/Abstract] AND gonadal[Title/Abstract] AND inhibition[Title/Abstract]), 45 results;

(dorsomedial hypothalamic nucleus[Title]), 23 results;

(RFRP3 Neurons[Title]), 57 results;

(kisspeptin neurons[Title] AND review[Title/Abstract]), 15 results;

(GABA[Title] AND glutamate[Title] AND neurons[Title/Abstract] AND review[Title/Abstract]), 23 results;

(CRH[Title] AND review[Title/Abstract]), 44 results;

(GnRH[Title] AND review[Title]), 121 results;

(circadian[Title] AND hypothalamic[Title]), 206 results;

(glucocorticoids[Title] AND stress[Title] AND review[Title/Abstract]); 54 results;

(gonadal hormones[Title] AND review[Title/Abstract]), 38 results;

(cortisol[Title] AND progesterone[Title] AND stress[Title/Abstract]), 26 results;

(human stress response[Title]), 21 results;

(biological feedback loops[Title]), 256 results;

(dynamical systems[Title] AND bifurcation[Title/Abstract]), 61 results;

((oscillations[Title] OR oscillatory[Title]) AND physiological[Title]), 71 results.

Titles and abstracts were screened for relevance, and reference lists of included articles were also examined to identify additional relevant studies. To address specific contextual issues relevant to the present work, a set of papers previously published by some of the authors (B.B. and I.D.) were also included. Based on this survey, we constructed an interaction map of the main physiological systems involved in the double-inhibitory interplay between the HPA and HPG axes.

2.2. Mathematical Model

The interaction map was formalized as a system of nonlinear ordinary differential equations (ODEs), representing nodes (variables) and directed edges (interactions). Loops, defined as closed chains of interactions, were explicitly modeled to capture recurrent feedback dynamics. The model was implemented in MATLAB R2025a (MathWorks, Natick, MA, USA) and expressed as a set of coupled ODEs having the general form: $\left\{\dot{X}\right\} = f(X)$

where X is a vector of variables, and $\dot{X}$ denotes their time derivative.

Symbolic definitions of interaction functions were coded and numerically solved using MATLAB's built-in solvers (e.g., ode45). Additional MATLAB routines were employed to perform parameter scans and to visualize trajectories, phase portraits, and bifurcation-like behaviors of the loop systems.

3. Results

3.1. Model Construction

3.1.1. Neuroendocrine Mechanisms of the HPA-HPG Inhibition

Based on the literature data, we reconstructed the mutual repression of HPA and HPG axes in the form of a series of interactions among hormones produced by adrenals and gonads and different hypothalamic districts. Repression of the HPA axis is due to inhibitory activities exerted by estrogens, androgens, progesterone, and their metabolites on neurons of the hypothalamic peri-paraventricular and paraventricular nuclei, and the anterior pituitary. Repression of the HPG axis is due to inhibitory activities exerted by corticosteroids on hypothalamic kisspeptin and gonadotropin-releasing-hormone (GnRH) neurons, the anterior pituitary, and gonads [19].

The HPA and HPG systems are traditionally referred to as axes but would be more accurately defined as networks. Their mutual inhibition is mediated by direct hormonal effects, along with GABAergic and glutamatergic neurotransmission. On the HPG axis side, this process involves hypothalamic GnRH and kisspeptin neurons in the preoptic area (POA) and arcuate nucleus (ARC) [20] (Figure 1). These neurons are the main target of feedback signaling by estradiol, which is considered the principal regulator of gonadotropin release. Negative feedback from estradiol on ARC kisspeptin neurons induces small, pulsatile releases of GnRH and LH. Conversely, positive feedback signaling from estradiol on POA kisspeptin neurons is responsible for the large surge of GnRH and LH that precedes ovulation [21]. However, both GnRH and kisspeptin neurons also express various types of glutamate and GABA receptors and respond to these neurotransmitters [22,23]. Multiple studies suggest that the LH surge is stimulated by glutamate [24,25], and inhibited by GABA [26,27], with its occurrence corresponding to a decrease in GABAergic transmission to both POA kisspeptin and GnRH neurons [28,29].

The effect of stressors reverberates on the HPG axis through repression induced by CRH and its CRH-R1 and CRH-R2 receptors, possibly acting via GABA neurons [30]. Moreover, cortisol can also inhibit the HPG axis by acting on hypothalamic nuclei and the pituitary [31]. It should be noted that stimulatory effects of CRH via CRH-Rs have also been observed under certain circumstances, suggesting stress biphasic effects on the HPG axis which overall induce dysregulation of reproductive activities [32].

Regarding the HPA axis, GABAergic and glutamatergic regulation occurs at the level of CRH neurons in the paraventricular nucleus (PVN) of the hypothalamus [33,34] (Figure 1). CRH neurons are activated by glutamate and inhibited by GABA, which binds to both synaptic and extra-synaptic GABA-A receptors, thereby mediating both phasic and tonic inhibition, respectively [35]. CRH release is also modulated by noradrenergic inputs from the brainstem. As a result, GABAergic transmission to CRH neurons can be either inhibited or enhanced, while glutamatergic signaling to CRH neurons is facilitated [36]. The activation of the HPA axis by psychosocial stressors involves complex polysynaptic pathways linking brain regions, such as the hippocampus, amygdala, and prefrontal cortex, to CRH neurons through multiple relays, including the bed nucleus of the stria terminalis, the medial preoptic area, and peri-paraventricular neurons, among others. These mechanisms allow for the downregulation of the stress response via inputs from the hippocampus and prefrontal cortex, whereas activation of the amygdala reduces GABAergic inhibition and stimulates the stress response [37].

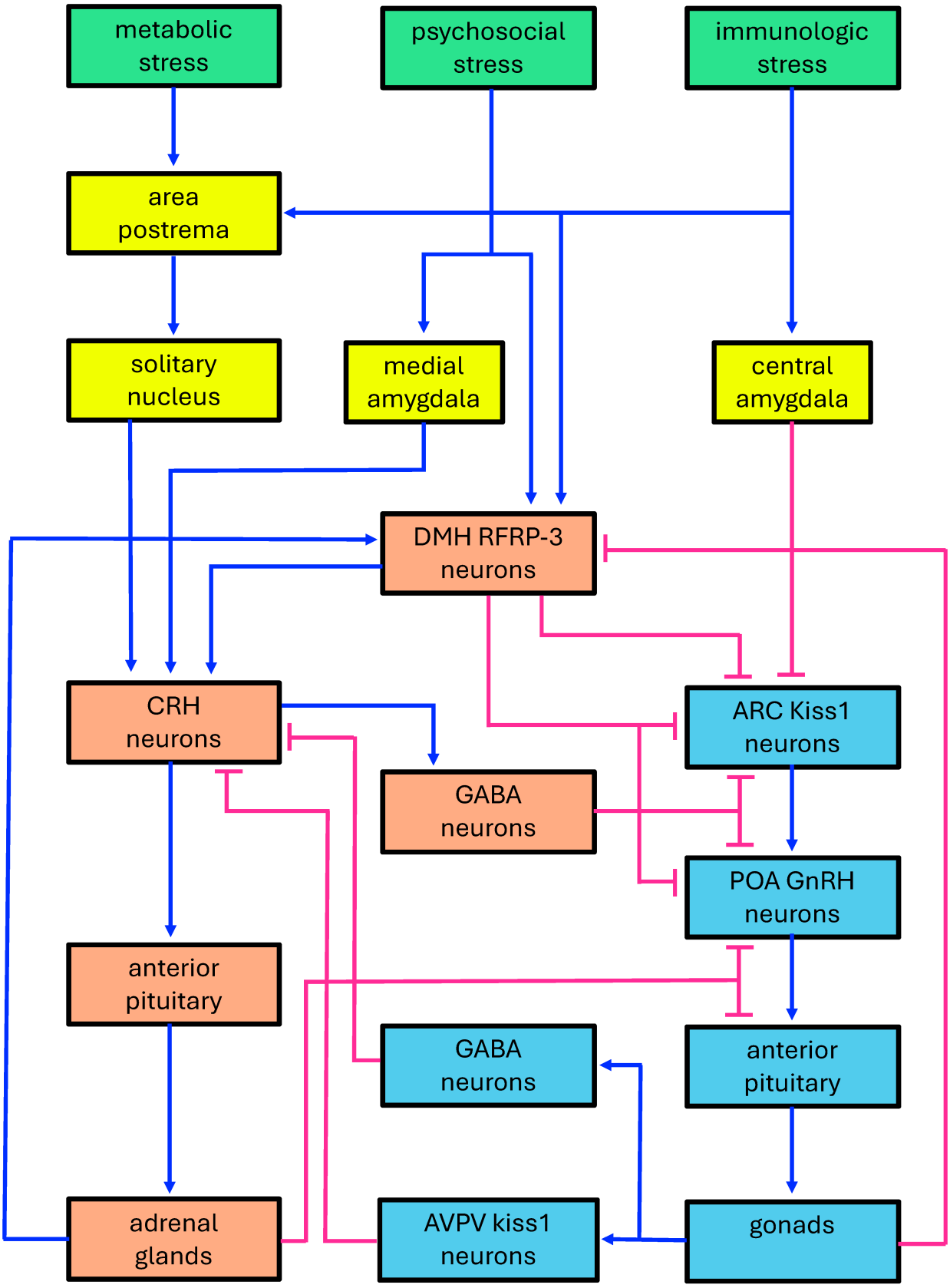

Figure 1. Diagram of the double-inhibitory system formed by the HPA and HPG axes. Green boxes: stress-inducing agents; yellow boxes: major neural districts mediating the effects of stress-inducing agents; orange boxes: neuroendocrine districts involved in the HPA axis; cyan boxes: neuroendocrine districts involved in the HPG axis. ARC: hypothalamic arcuate nucleus;

AVPV: hypothalamic anteroventral periventricular nucleus; CRH: corticotropin-releasing hormone; DMH: dorsomedial hypothalamic nucleus; GABA: gamma-aminobutyric acid; GnRH: gonadotropin releasing hormone; kiss1 neurons: kisspeptin neurons; POA: hypothalamic preoptic area; RFRP3: (Arg)(Phe) related peptide-3. Blue lines: activations; pink lines: inhibitions.

The influence of the HPG axis on HPA activity partly depends on neurosteroids, mainly allopregnanolone. This latter is synthesized in the brain but is a metabolite of progesterone and its brain level shows a positive correlation with high plasma rises of its gonadal precursor [11]. Allopregnanolone is known to positively modulate GABA-A receptors, thereby repressing the HPA stress response [38]. In mice, it has been found that kisspeptin neurons in the anteroventral periventricular nucleus (AVPV) of the hypothalamic preoptic area send inhibitory GABAergic projections to the hypothalamic paraventricular (PVN) and dorsomedial hypothalamic (DMH) nuclei [39]. Moreover, it has been observed in vitro that rat PVN cells express less CRH when treated with kisspeptin [40].

In this context, the hypothalamic DMH plays a significant role through neurons that release RFamide-related peptide-3 (RFRP-3). This nucleus serves as a critical junction between stress-inducing factors and the reciprocal interaction of the HPG and HPA axes. RFRP-3 neurons stimulate the HPA axis while inhibiting the HPG axis [41]. Additionally, they receive stimulatory feedback from the HPA axis, mediated by glucocorticoids, which contributes to the stress-induced suppression of reproduction [42,43]. Conversely, RFRP-3 neurons are subject to inhibitory feedback from the HPG axis, primarily mediated by estradiol [44–46], but also by kisspeptin neurons from the preoptic area [47] (Figure 1).

3.1.2. Increasingly Expanded Interaction Maps

Given the pathways thought to play key roles in the HPA-HPG interaction, we developed progressively expanded versions of the system to enable computational analysis. These versions allowed us to test the robustness of our model and to identify the key bifurcation parameters that most strongly influence the system's behavior.

The most schematic version consists of a tripartite loop, comprising three interconnected feedback loops arranged in a closed chain (Figure 2a). A substantial amount of data on the input–output relationships among endocrine systems suggests that endocrine axes can be viewed as a monotonic collection of subsystems [11]. Thus, from a mathematical standpoint, these subsystems can be treated as a collapsed single element within a mathematical model of the dynamic system under consideration. This approach still enables the analysis of its behavior by examining the presence of signed loops [48]. Based on these premises, to model the dual inhibition of the two axes, we employed a system comprising three variables: one (X1) represents the collapsed HPA axis network, the second (X2) corresponds to the collapsed HPG axis, and the third (X3) reflects the activity of RFRP-3 neurons in the DMH nucleus. This latter element cannot be condensed within the collapsed HPA or HPG axes because it establishes reciprocal activation with HPA and reciprocal inhibition with HPG. As such, it cannot be integrated into the cascade of activations with negative feedback, typical of either axis. It must therefore be represented as a distinct variable to fully describe the system. Additionally, we introduced self-limiting components for each variable, reflecting the biological principle that the growth or increase in a variable limits its own future growth. Self-limiting parameters were also used for all variables in the following versions of the system.

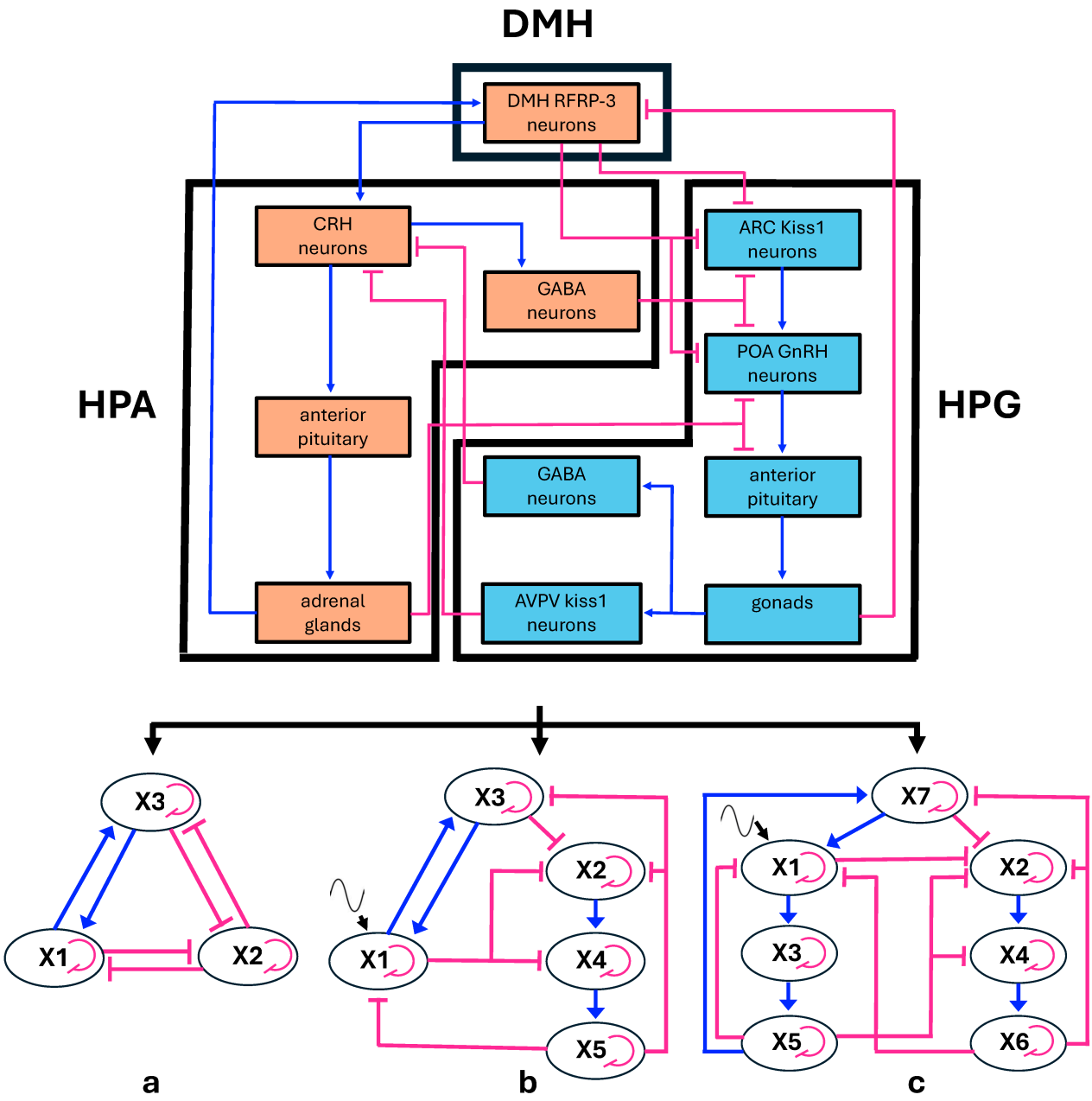

Figure 2. (**Top**) Diagram showing the relationships among the endocrine axes and the DMH nucleus (acronyms as in Figure 1). (**Bottom**) From this configuration, three schematic multiple-loop models were derived as follows: (**a**) simple tripartite system in which both the HPG and HPA axes are condensed into single elements; (**b**) model derived from (**a**), with the HPG axis expanded into three components and a sinusoidal input added to the HPA axis; (**c**) model derived from (**b**), in which the HPA axis is also expanded into three components, while the sinusoidal input is retained. The elements of the multiple-loop models are labeled with the names of the variables used in the corresponding differential equation systems. The biological counterparts of variables are the following: (**a**) *X1* = HPA axis condensed, *X2* = HPG axis condensed, X3 = DMH RFRP3 neurons, (**b**) *X1*: condensed HPA axis, *X3* = DMH RFRP3 neurons, *X2* = ARC Kiss and POA GnRH neurons, *X4* = anterior pituitary LH and FSH cells, *X5* = gonadal progesterone cells; (**c**) X1 = PVN CRH neurons, *X3* = anterior pituitary ACTH cells, *X5* = adrenal cortisol cells, *X2* = ARC Kiss neurons and POA GnRH neurons, *X4* = anterior pituitary LH and FSH cells, *X6* = gonadal progesterone cells, *X7* = DMH RFRP3 cells (see also Box 1 in the Mathematical Modeling section). Blue lines: activations; pink lines: inhibitions, fine pink curved lines: self-limitation effects, fine black wavy lines: sinusoid input to HPA axis.

The second version of our system accounts for oscillatory behavior (Figure 2b). Plasma levels of glucocorticoids and gonadal hormones show ultradian, circadian, and long-term fluctuations, revealing oscillatory functioning of endocrine systems. As said above, the mutual interaction between the HPA and HPG axes becomes significant for stronger oscillations of either axes, and therefore we dismissed smaller ultradian fluctuations. This led us to consider main circadian oscillations of the HPA axis, which are principally regulated by the circadian clock residing in the hypothalamic suprachiasmatic nucleus (SCN) [49]. To model this mechanism, we used a sinusoid oscillatory input. Conversely, in modeling the oscillations of the HPG axis, our focus was primarily on progesterone, as both the hormone itself and its neurosteroid derivatives exert strong negative feedback on hypothalamic centers [11]. In this context, we disregarded smaller ultradian and circadian oscillations, considering only the 28-day female menstrual cycle. Progesterone fluctuations over the cycle can be approximated by a sinusoidal function and are largely driven by negative feedback on the hypothalamic and pituitary components of the axis [50]. To capture the oscillatory behavior of the HPG axis, we expanded the model to include its three main components, namely the hypothalamic, pituitary, and gonadal regions, forming a negative feedback loop.

Finally, we also analyzed a third version where we also expanded the HPA axis into its hypothalamic, pituitary, and adrenal components, arranged to form one negative feedback as seen above for the HPG axis (Figure 2c). In this version, we maintained the sinusoidal input to the HPA axis representing the SCN circadian clock effect.

Box 1. ODE systems in the three versions of the HPA-HPG inhibition model.

ODE system 1 (condensed HPA and HPG axes)
Variables: *X1* = HPA axis condensed; *X2* = HPG axis condensed; *X3* = DMH RFRP3 neurons
Parameters: h_n = hill exponent, e_n = response threshold, and p_n = self-limitation parameter of neural elements
h_d = hill exponent, e_d = response threshold, and p_d = self-limitation parameter of endocrine elements
Combined interactions:
noncompetitive (single activation and single inhibition): $\frac{X_i^{h_i}}{e_i^{h_i}+X_i^{h_i}} \cdot \frac{1}{1+\left(\frac{X_j}{e_j}\right)^{h_j}}$
(generic indices)
competitive double inhibition: $\frac{1}{1+\left(\frac{X_i}{e_i}\right)^{h_i}+\left(\frac{X_j}{e_j}\right)^{h_j}}$
ODE system:

$$\dot{X}_1 = \frac{X_3^{h_n}}{e_n^{h_n}+X_3^{h_n}} \cdot \left(1 - \frac{X_2^{h_d}}{e_d^{h_d}+X_2^{h_d}}\right) - p_d \cdot X_1$$

$$\dot{X}_2 = \frac{1}{1+\left(\frac{X_1}{e_d}\right)^{h_d}+\left(\frac{X_3}{e_n}\right)^{h_n}} - p_d \cdot X_2$$

$$\dot{X}_3 = \frac{X_1^{h_d}}{e_d^{h_d}+X_1^{h_d}} \cdot \left(1 - \frac{X_2^{h_d}}{e_d^{h_d}+X_2^{h_d}}\right) - p_n \cdot X_3$$

ODE system 2 (expanded HPG axis)
Variables: *X1*: condensed HPA axis
X2, *X4*, *X5*: HPG axis
X2 = ARC Kiss and POA GnRH neurons
X4 = anterior pituitary LH and FSH cells
X5 = gonadal progesterone cells
X3 = DMH RFRP3 cells
Parameters: see above, and in addition, ω = frequency of the sinusoid input, and A = amplitude of the
sinusoid input.

Box 1. *Cont.*

ODE subsystem for sinusoid input: $\dot{X}_{circ_1} = \omega \cdot X_{circ_2}$

$\dot{X}_{circ_2} = -\omega \cdot X_{circ_1}$

oscillation imposed to HPA by the SCN (circadian clock)

Combined interactions:

noncompetitive (single activation and single inhibition): see above

competitive multiple inhibition: $\frac{1}{1+\left(\frac{X_i}{e_i}\right)^{h_i}+\left(\frac{X_j}{e_j}\right)^{h_j}+\ldots}$

ODE system:

$$\dot{X}_1 = \frac{X_3^{h_n}}{e_n^{h_n}+X_3^{h_n}} \cdot \frac{1}{1+\left(\frac{X_5}{e_d}\right)^{h_d}} - p_d X_1 + A \cdot \left(X_{circ_1}+1\right)$$

$$\dot{X}_2 = \frac{1}{1+\left(\frac{X_1}{e_d}\right)^{h_d}+\left(\frac{X_3}{e_n}\right)^{h_n}+\left(\frac{X_5}{e_d}\right)^{h_d}} - p_n X_2$$

$$\dot{X}_3 = \frac{X_1^{h_d}}{e_d^{h_d}+X_1^{h_d}} \cdot \frac{1}{1+\left(\frac{X_5}{e_d}\right)^{h_d}} - p_n X_3$$

$$\dot{X}_4 = \frac{1}{1+\left(\frac{X_1}{e_d}\right)^{h_d}} \cdot \frac{X_2^{h_n}}{e_n^{h_n}+X_2^{h_n}} - p_d X_4$$

$$\dot{X}_5 = \frac{X_4^{h_d}}{e_d^{h_d}+X_4^{h_d}} - p_d X_5$$

ODE system 3 (expanded HPG and HPA axes)

Variables: *X1*, *X3*, *X5*: HPA axis

X1 = PVN CRH neurons

X3 = anterior pituitary ACTH cells

X5 = adrenal cortisol cells

X2, *X4*, *X6*: HPG axis

X2 = ARC Kiss neurons and POA GnRH neurons

X4 = anterior pituitary LH and FSH cells

X6 = gonadal progesterone cells

X7 = DMH RFRP3 cells

Parameters: see above

Combined interactions: see above, and in addition, noncompetitive interaction between single activation and competitive multiple inhibition = $\frac{X_i^{h_i}}{e_i^{h_i}+X_i^{h_i}} \cdot \frac{1}{1+\left(\frac{X_j}{e_j}\right)^{h_j}+\left(\frac{X_k}{e_k}\right)^{h_k}+\ldots}$

ODE system:

$$\dot{X}_1 = \frac{X_7^{h_n}}{e_n^{h_n}+X_7^{h_n}} \cdot \frac{1}{1+\left(\frac{X_5}{e_d}\right)^{h_d}+\left(\frac{X_6}{e_d}\right)^{h_d}} - p_n X_1 + A \cdot \left(X_{circ_1}+1\right)$$

$$\dot{X}_2 = \frac{1}{1+\left(\frac{X_1}{e_n}\right)^{h_n}+\left(\frac{X_5}{e_d}\right)^{h_d}+\left(\frac{X_6}{e_d}\right)^{h_d}+\left(\frac{X_7}{e_n}\right)^{h_n}} - p_n X_2$$

$$\dot{X}_3 = \frac{X_1^{h_n}}{e_n^{h_n}+X_1^{h_n}} - p_d X_3$$

$$\dot{X}_4 = \frac{X_2^{h_n}}{e_n^{h_n}+X_2^{h_n}} \cdot \frac{1}{1+\left(\frac{X_5}{e_d}\right)^{h_d}} - p_d X_4$$

$$\dot{X}_5 = \frac{X_3^{h_d}}{e_d^{h_d}+X_3^{h_d}} - p_d X_5$$

$$\dot{X}_6 = \frac{X_4^{h_d}}{e_d^{h_d}+X_4^{h_d}} - p_d X_6$$

$$\dot{X}_7 = \frac{X_5^{h_d}}{e_d^{h_d}+X_5^{h_d}} \cdot \frac{1}{1+\left(\frac{X_6}{e_d}\right)^{h_d}} - p_n X_7$$

3.1.3. Mathematical Modeling

To carry out computational analyses of the above versions of the HPA-HPG interaction, we defined three systems of ordinary differential equations (ODEs), where the dynamics of each variable are described based on its interactions with the other variables.

The effects of a variable on another variable were described using Hill functions, increasing ones for activating effects, and decreasing ones for inhibitory effects. This choice is generally adopted for a wide series of nonlinear biological input–output processes [51], notably for endocrine and neuron interactions (see also the literature surveys in [11,52]). In addition, in our schematic models, different variables receive more than one input. To model such combined influences, noncompetitive interactions, i.e., noncompeting for the same binding site or mechanism, were assumed for combined activating and inhibitory actions. Conversely, competitive interactions, i.e., competing for the same binding site or regulatory pathway, were assumed for combined inhibitory actions, because the inhibitory pathways considered in our study are mediated by GABAergic transmission (see above the "Neuroendocrine Mechanisms of the HPA-HPG Inhibition" section). Noncompetitive interactions were modeled as the product of Hill functions, while competitive interactions were modeled additively (see below for details). This kind of mathematical modeling is widely used in fields like biochemistry, gene regulation, and systems biology [53–55].

As reported in a previous survey [11], and summarized above, the reciprocal inhibitory effects between the HPA and HPG axes become evident when either axis enhances its activity beyond daily fluctuations. This behavior is intrinsically modeled by the Hill function which describes a situation where a variable responds in an ultrasensitive manner to changes in the input variable, characterized by a steep transition from low to high (or high to low) response as the input variable crosses a certain threshold. The threshold parameter in the Hill function typically represents the concentration or value at which the response reaches half of its maximum and was denoted by e in our ODEs. The ultrasensitivity is represented by the steepness or ultrasensitive nature of the response, controlled by the Hill coefficient, denoted by h in our ODEs. The values assigned to these parameters were derived from a previous literature survey [11]. The negative feedback exerted by each variable on itself was modeled by adding a self-limiting component pX, with negative sign, where the parameter p represents the weight of the self-limiting effect. The sinusoid input to HPA was modeled by adding an $A \cdot (X_{circ_1} + 1)$ component, where X_{circ_1} is part of an ODE subsystem with two variables: X_{circ_1} and X_{circ_2}, forming an independent harmonic oscillator, and A represents the amplitude. The addition of 1 to X_{circ_1} acts as an offset, ensuring that during ODE integration, the dependent variable does not fall below its lower bound of 0. The harmonic oscillator generates a perfect sinusoid when defined on the set where the equation is satisfied as follows: ${X^2}_{circ_1} + {X^2}_{circ_2} = 1$.

Based on the above considerations, three ODE systems were defined, each corresponding to one of the loop configurations shown in Figure 2. These represent three different versions of the model describing the mutual inhibition between the HPA and HPG axes. The systems of equations, along with the descriptions of their components, variables, and parameters, are presented in Box 1. The range of variables was set within the [0, 1] interval, in arbitrary units corresponding to 0 to 100% activity. The parameters of the Hill functions were set according to a previous study [11]. In the modeling of HPA oscillations, the parameter ω of the sinusoid input was set to simulate a higher frequency with respect to the HPG cycle, because HPG oscillations represents the approximately monthly female cycle, while those of HPA corresponds to the daily fluctuation of cortisol. The amplitude A was set based on the ratio between the daily plasma cortisol peak at arousal (the peak of the sinusoidal daily variation) and the corresponding peak during a stress response (the maximum possible value attained by the variable) [56,57]. The range of the variables and the values assigned to the parameters are detailed in Table 1.

Table 1. Symbols and quantities in the ODEs.

	Symbol	Assigned Range/Value	Quantity	Ref.
Variables	X_i	Scaled to $[0,\ 1]$	(see Box 1)	
	$X_{circ_1},\ X_{circ_2}$	$X^2{}_{circ_1} + X^2{}_{circ_2} = 1$	Variables of the harmonic oscillator generating a sinusoid trend	
Parameters	h_n	2.5	Hill coefficient of neuronal effects	[11]
	h_d	6	Hill coefficient of endocrine effects	[11]
	e_n	0.2	half-saturation constant of neuronal effects measuring the threshold of X_i inducing a significant response of X_j	[11]
	e_d	0.3	half-saturation constant of endocrine effects (see above)	[11]
	p_n	1	weight of the self-limiting effect in neuronal elements	
	p_d	1	weight of the self-limiting effect in endocrine elements	
	A	0.1, 0.2	amplitude of *HPA* oscillation	[57]
	ω	$5{\cdot}\pi$	frequency of *HPA* oscillation	

3.2. Computational Analysis of Phase Portraits and Bifurcation Patterns

We utilized MATLAB to characterize the dynamical landscape of our nonlinear model, including the identification of trajectories and, in the case of bistability, the decision boundary separating the basins of attraction. The term bistability is used here in a broad dynamical sense to denote the partitioning of an initially single basin of attraction into two distinct basins, each associated with its own attractor (see the Discussion section). The simplest tripartite system can exhibit either bistable or monostable behavior, depending on the choice of parameter values (Figure 3).

In the more complex versions, the expansion of HPG, or of both axes, together with the addition of a circadian input to HPA, converts stable equilibria into attractors exhibiting oscillatory behavior. Due to the sinusoidal input to the variable representing the condensed HPA axis, or to the hypothalamic component of the expanded HPA axis, the attractor is not a true limit cycle but rather a bundle of Lissajous curves, with each trajectory eventually settling on its own individual curve. These Lissajous curves arise from the combined oscillatory dynamics of the HPA and HPG axes. (Figure 3). Nevertheless, in the versions with expanded axes, the overall behavior with respect to mono- or bistability remains essentially unchanged. The trajectories in the phase space demonstrate that under bistability, HPG is always opposed to HPA and DMH at the attractors. Namely, when HPG is high, the other two are low, and vice versa (Figure 3).

We then performed a bifurcation analysis to examine how the ODE parameters influence the system's bifurcation structure within realistic value ranges. For each parameter, we conducted a separate analysis by varying its value while keeping the others fixed at the reference values reported in Table 1. The analysis reveals two mechanisms shaping the system's dynamics. In all versions of the model, bifurcations drive transitions from monostability to bistability, allowing the coexistence of distinct stable states (Figure 4). Moreover, when either axis is expanded, including its intrinsic negative feedback, Hopf-like bifurcations appear on the upper attractor (not genuine Hopf due to the oscillatory nature of the attractor) (Figure 4). This dual organization suggests that the system can exhibit both between-attractor transitions (switching between alternative stable states), and within-attractor changes in dynamical regime (fixed point oscillations), depending on bifurcation parameter values. Such a combination provides a rich repertoire of possible responses to perturbations and parameter modulation.

In the simple tripartite system, where oscillations are absent, saddle-node bifurcations (transitions between monostability and bistability) are observed only with p_d and p_n. In the two more complex versions of the system, in addition to the duplication of attractors due to p_d and p_n variations, transitions to bistability also occur with e_d, e_n, h_d, and h_n. These more complex versions are similar to each other in their bifurcation pattern, indicating that the expansion of the HPA axis has a very limited effect on the bifurcation structure of the system (Figure 4). Furthermore, we performed bifurcation analysis for the sinusoidal subsystem parameters A and ω, which showed no bifurcation pattern.

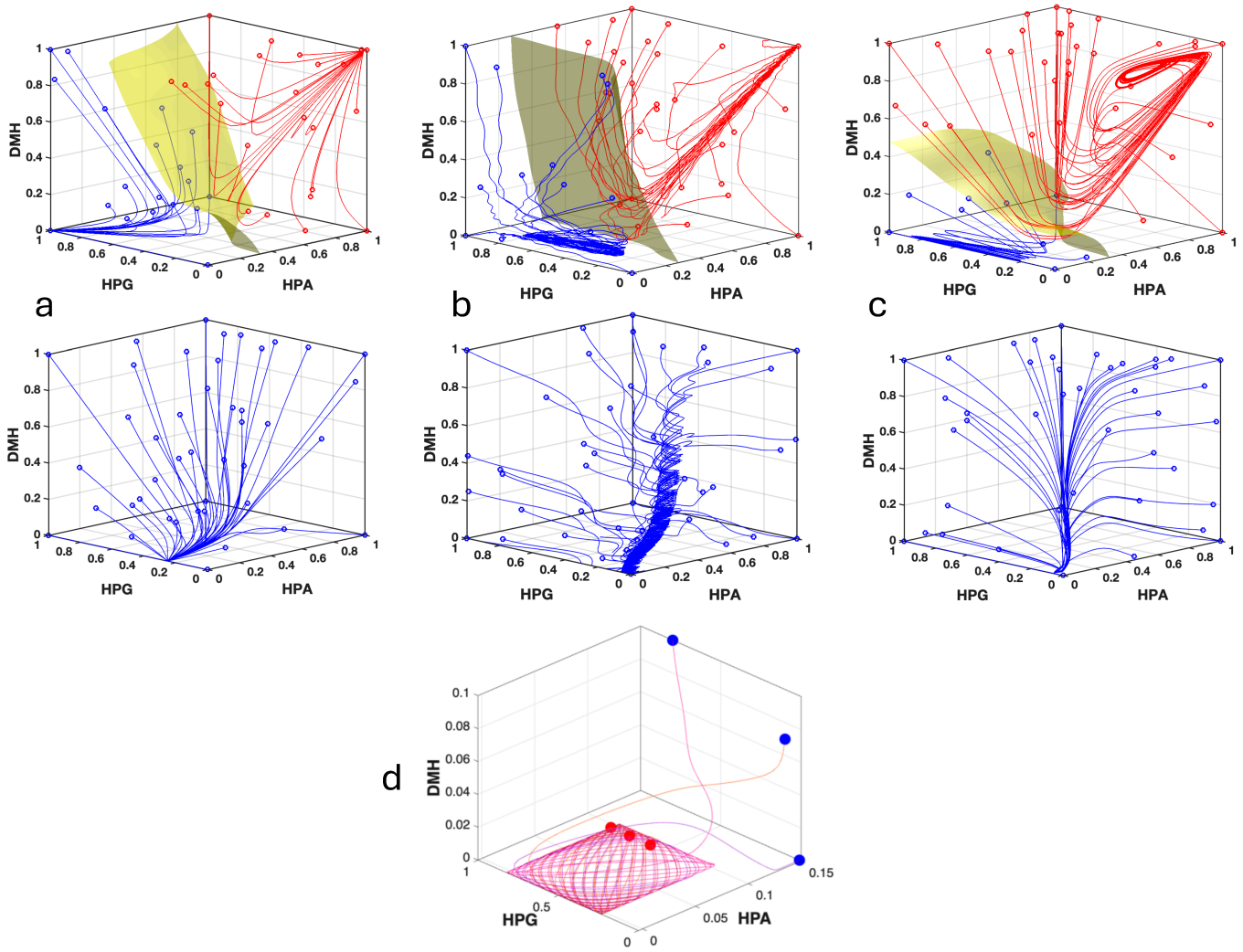

Figure 3. Phase portraits depicting the variation through time of the system variables in its three versions. (**a**) Phase portrait with different exemplificative trajectories of the simple tripartite system ($HPA = X_1$, $HPG = X_2$, $DMH = X_3$; see Figure 2a), The system shows bistability for $p_d = 1$ (upper panel), and monostability for $p_d = 4$ (lower panel). (**b**) Same as above for the system version with the HPG axis expanded ($HPA = X_1$, $HPG = X_5$, $DMH = X_3$; trajectories initialized with $(X_2, X_4) = (0.4, 0.4)$; see Figure 2b). (**c**) Same as above with both axes expanded ($HPA = X_5$, $HPG = X_6$, $DMH = X_7$; trajectories initialized with $(X_1, X_2, X_3, X_4) = (0.05, 0.05, 0.05, 0.05)$; see Figure 2c). (**d**) Detail of the phase portrait in (**b**) showing three trajectories converging to an oscillatory attractor composed of a bundle of Lissajous curves. Blue dots indicate initial points, red dots indicate final points.

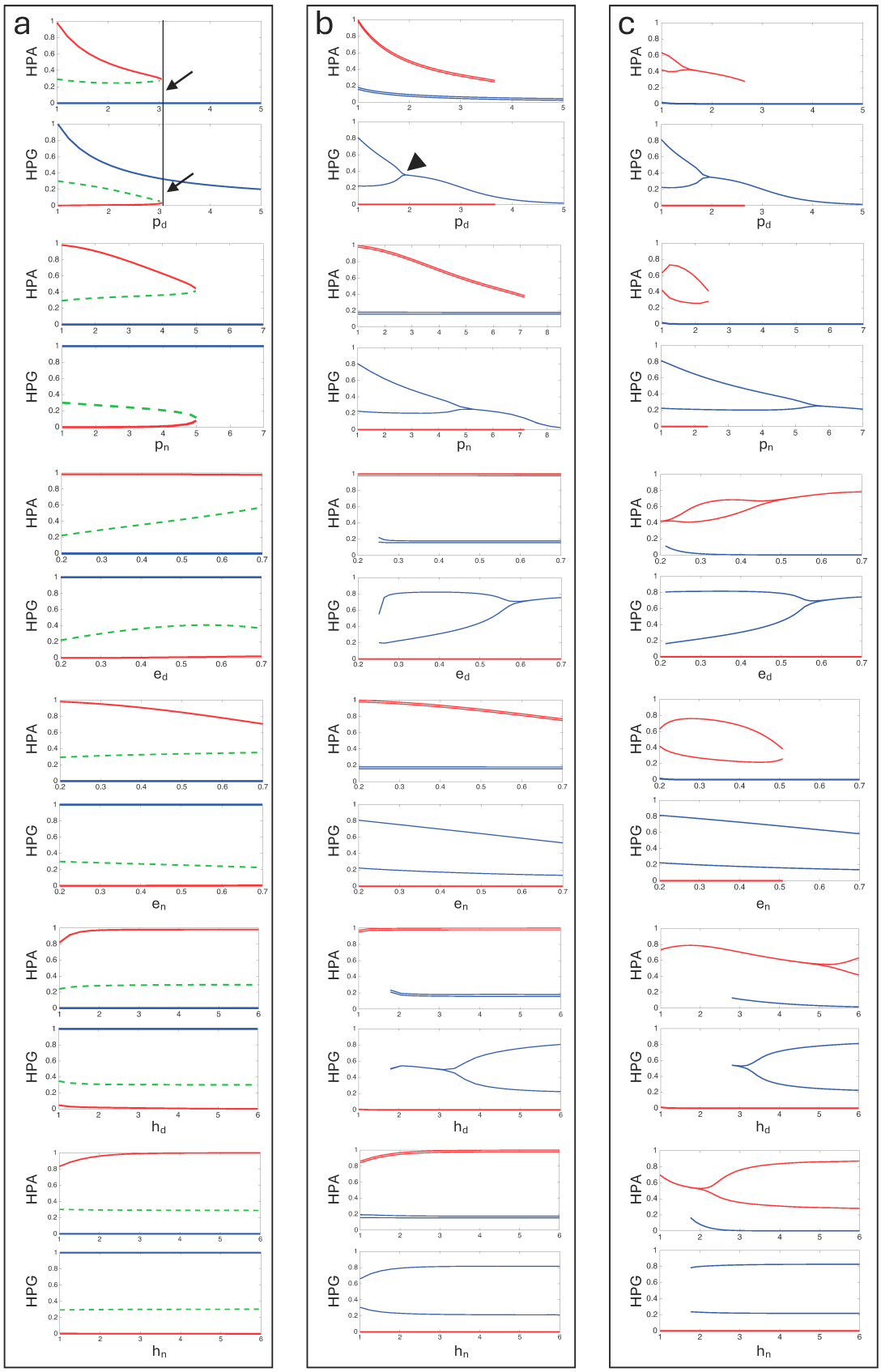

Figure 4. Bifurcation diagrams of the ODE systems for the three model versions (see Figures 2 and 3), illustrating how equilibrium values or attractor oscillations change as a function of different bifurcation parameters. (**a**) Simple tripartite system. For each parameter, two bifurcation diagrams are shown corresponding to the variables $HPA = X_1$ and $HPG = X_2$. Solid lines represent stable equilibria, while dashed lines indicate unstable equilibria. Colors distinguish the different attractors.

(**b**) System with expanded HPG axis and sinusoid input to the HPA axis. Diagrams are shown as in (**a**) ($HPA = X_1$ *and* $HPG = X_5$). Attractors exhibiting oscillatory behaviour are represented by pairs of lines indicating the maximum and minimum values of the variable within the attractor. Unstable equilibria were not calculated. (**c**) System with expanded HPG and HPA axes and sinusoid input to HPA axis. Diagrams are shown as in (**b**) ($HPA = X_5$ and $HPG = X_6$). Some diagrams show saddle-node bifurcations (transitions between monostability and bistability, e.g., bifurcation point indicated by arrows and vertical line). In some cases, Hopf-like bifurcations are visible (e.g., arrowhead).

We finally explored the relationships among the bifurcation parameters in inducing bistability, focusing on the system with an expanded HPG axis and sinusoidal input to the HPA axis. Three-dimensional cube diagrams, with axes representing triplets of parameters, showed that parameters are correlated in promoting bistability (Figure 5). When more parameters vary simultaneously, the system is more prone to bistability for decreasing values of p_d and p_n (reflecting the strength of the self-limiting effect), decreasing values of e_d and e_n (the half-saturation constants), and for increasing values of h_d and h_n (the Hill coefficients). In summary, the bifurcation analysis indicates that bistability generally arises from increased hypersensitivity and sustained system activity.

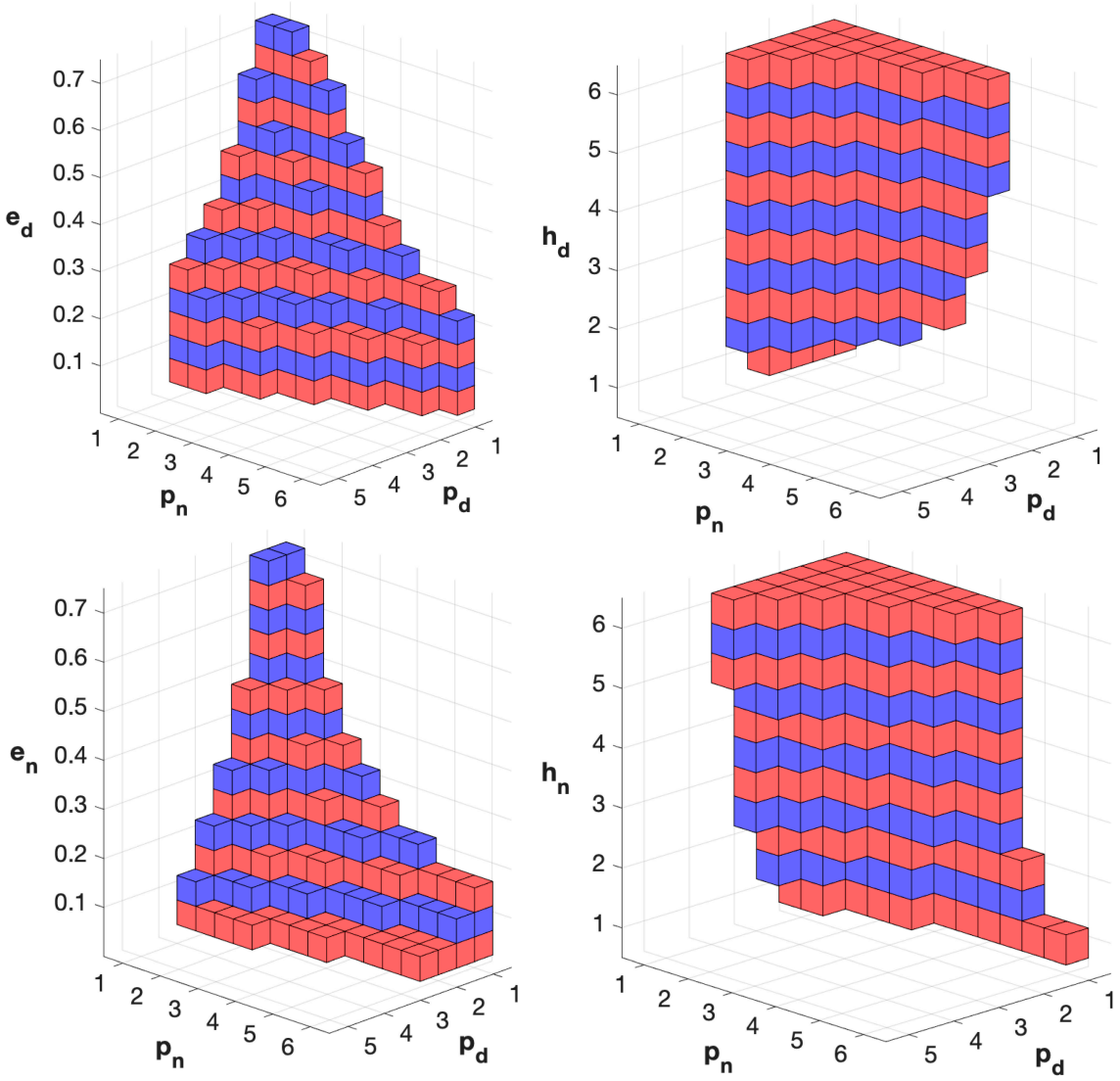

Figure 5. Analysis of the relationships among bifurcation parameters in the model version with HPG axis expanded and sinusoid input to HPA axis. The diagram shows the occurrence of bistability for

triplets of values of the bifurcation parameters. The axis labels indicate the parameter values used to generate the triplets. Colored cubes indicate bistability for the corresponding triplet, while the absence of a cube indicates monostability. Alternated colors are used to enhance the visibility of the ladder-shaped arrangement.

4. Discussion

4.1. Interpretation of the Results and Their Possible Application

Our modeling approach assumes that closed-chain interactions represent a fundamental and essential feature of biological functioning. This kind of modeling is assumed to be the most efficient way to acquire control of life systems [2]. Accordingly, our goal is to develop a coherent model of the HPA and HPG axes and to demonstrate its relevance in medical and clinical contexts. The first point to consider is that our study primarily aims to identify patterns rather than focus on the absolute values of the mathematical results. In the ODE systems used to model the HPA-HPG interaction, parameter values were derived from the literature data on a statistical basis and serve as schematic approximations. Conversely, the pattern of interactions could be affordably reconstructed from the literature data. As a result, the numerical outcomes of our computational analyses should not be interpreted as accurate reproductions of the activities of the actual biological systems. Instead, our primary interest lies in the system's qualitative behavior, specifically, its propensity for bistability, the occurrence of bifurcations, and the identification of bifurcation parameters. This focus aligns with the idea previously formulated by one of us, stating that, in modeling biological processes that underlie functional changes, whether physiological or pathological, the parameters driving bifurcations can be considered critical targets for system control [58].

The first general result observed in our computational analysis was the system's ability to transition from having a single basin of attraction to having two distinct basins of attraction. This cannot always be described strictly as a transition from monostability to bistability, since the system may converge to an oscillatory attractor rather than a fixed point. However, the presence of multiple stable attractors (either oscillatory ones or fixed points) is sufficient to qualify it as bistability in a broader dynamical sense [59]. In our case, for certain parameter values, the system reliably converges to a single regime of functioning, irrespective of initial conditions. When these parameters are varied, the system develops the possibility of evolving toward one of two distinct functional regimes, depending on initial conditions, consistent with the definition of bistability involving coexisting attractors [60].

Building on a range of data from the literature, one of us previously developed the idea that bistability, or more broadly multistability, is a fundamental prerequisite for any form of endogenous change in living systems, including the emergence of pathological conditions [58]. Accordingly, a key finding of our analysis was the identification of bifurcation parameters. The trajectories produced by the system, along with the bifurcation behavior, exhibited a distinct uniformity across the different model variants representing the HPA-HPG interaction. The consistency of these results suggests their reliability in representing the actual behavior of the modeled biological system. Even the introduction of oscillatory components, which changed the nature of bifurcations, did not substantially alter the pattern.

In all versions of the model, the parameters p_d and p_n, which quantify the strength of the self-limiting mechanisms, consistently acted as bifurcation parameters. Bifurcations invariably arose as the influence of these self-limiting components decreased, indicating that the system becomes bistable when its components are more capable of sustaining high levels of activity in response to activating stimuli. Moreover, in all cases and for all vari-

ables, bifurcation involved a transition from a single low-activity attractor to two distinct attractors, including the emergence of a new high-activity state. This shift suggests a potential breakdown of homeostatic control.

In the fully expanded version of the model, additional bifurcations were observed with decreasing values of e_n and increasing values of h_d. A reduction in e_n corresponds to a lower activation threshold for stimuli exerted by neural elements, while an increase in h_d reflects heightened hypersensitivity to endocrine stimuli, with responses becoming sharply concentrated around the input threshold. Overall, the bifurcations identified in our analysis consistently point to mechanisms involving increased sensitivity and responsiveness of the system's components to the received stimuli. In particular, regarding p_d, it is well known that the primary self-limiting mechanism for the homeostatic control of an endocrine axis is negative feedback. Therefore, the mechanisms governing negative feedback represent potential therapeutic targets for the diseases whose insurgence can be represented by certain functional states of our model. These include, for instance, stress-related disorders (characterized by hyperactivity of the HPA axis) with higher female prevalence (involving the HPG axis and significant fluctuations in female gonadal hormones) [11].

It is well known that stress-related psychiatric disorders such as depression, post-traumatic stress disorder (PTSD), and anxiety show a higher prevalence in females than in males [61,62]. It has been proposed that, in these conditions, the inability to appropriately terminate the stress response leads to a heightened sensitivity to stressors [63], mainly due to a failure of glucocorticoid-mediated negative feedback on the HPA axis, largely attributable to impaired glucocorticoid receptor (GR) function [64]. GRs are central mediators of the negative feedback regulation of the HPA axis. These low-affinity receptors are activated by elevated concentrations of circulating glucocorticoids, such as those occurring during the circadian peak or in response to stress. GRs are widely expressed throughout the brain, including the hippocampus, prefrontal cortex, amygdala, and the hypothalamic PVN, all regions critically involved in the regulation of HPA axis negative feedback [65]. Overall, evidence from the literature underscores that proper regulation of GR function is critical for maintaining homeostatic HPA axis activity, while various impairment mechanisms have also been highlighted. These latter involve impaired GR expression [66,67], nuclear translocation [68], and serine phosphorylation [69].

In the framework of our model of HPA-HPG interactions, GRs can be associated with the p_d bifurcation parameter and thus can be suggested as potential therapeutic target for stress- and sex-related disorders, for which effective treatments are still lacking or insufficient. This approach could be highly effective, due to its ability to target the modulatory mechanisms of pathogenic dynamics. However, since GRs are expressed in multiple tissues, systemic targeting would produce broad metabolic and anti-inflammatory effects. Therefore, to precisely modulate the dynamics of the HPA–HPG interaction for therapeutic purposes, selective techniques should be employed to directly access hypothalamic areas or to drastically reduce side effects, such as nanotechnology, intranasal delivery routes, or the promising selective glucocorticoid receptor modulators (SGRMs) [70].

Representative examples of disorders linked to HPA-HPG impairment include post-partum depression (PPD), in which reduced levels of allopregnanolone lead to impaired GABAergic neurotransmission, which in turn contributes to HPA axis hyperactivation [38]. Clinical trials have shown that treatment with allopregnanolone analogues effectively alleviates PPD symptoms [71,72]. Moreover, psychological distress and elevated cortisol levels have been identified as predictive risk factors for the onset of PPD symptoms [73,74], supporting the rationale for investigating new therapeutic targets within the molecular mechanisms regulating HPA axis feedback, particularly through modulation of GR activity. Fibromyalgia is another stress-related syndrome with a markedly higher prevalence in

females. It is characterized by chronic pain accompanied by fatigue and sleep disturbances, but the etiopathogenesis is unknown and effective treatments are lacking. In a previous paper, some of us proposed a pathogenic model of fibromyalgia considering the mutual HPA-HPG inhibition [11]. Based on this hypothesis, we suggested that treatment with allopregnanolone analogues could represent a promising treatment strategy for fibromyalgia [75]. Furthermore, the results from the present study indicate the modulation of GR activity as a foundation for a novel therapeutic hypothesis.

4.2. Limitation of the Study

This study is fundamentally based on the Loopomics hypothesis, which posits that every biological process, metabolic pathway, and regulatory mechanism arises from the dynamics of closed chains of interactions, admitting regular (non-chaotic) attractors [2]. This perspective extends and generalizes various ideas and approaches developed in systems biology [3], and represents a completely new vision of life, in which the modeling of interaction patterns provides the key to developing interventional strategies. More specifically, the hypothesis implies that pathogenic processes underlying a wide range of human diseases can be modeled by a restricted family of positive loop systems admitting bi- or low-dimensional stability, where bifurcation parameters define the ultimate therapeutic targets [58].

This interpretation of life addresses fundamental issues, such as the absence of butterfly effects in biological processes and their high predictability, despite the astonishing number of chemical reactions and physical processes involved, each with a proportional contribution from noisy components. However, the Loopomics hypothesis has not yet received experimental support. Persuasive evidence could come from the discovery of at least a partial solution to one of the many still intractable diseases, particularly those that have been the focus of great and prolonged efforts without producing any significant clinical improvement. At present, the validity of the hypothesis remains limited to its adherence to fundamental life features and the ease of identifying loops in metabolic pathways from available data. This includes positive loops in pathogenic processes and a unifying and well-defined analytical approach for disease management. The contents of this study and their potential applications fully share both the innovative strengths and the limitations of the underlying theoretical framework.

5. Conclusions

We presented a mathematical description of the HPA-HPG complex using a system of ODEs that captures its closed-loop interactions. The model exhibits a transition to bistability for specific values of parameters associated with increased hypersensitivity and excitability. Various findings from the literature suggest that our analysis may be relevant to a range of stress- and sex-related disorders whose pathogenesis and treatment remain to be fully understood. In this context, the bifurcation parameters identified in our model could help guide biomedical and pharmacological research toward more effective therapeutic targets.

Author Contributions: Conceptualization, B.B. and I.D.; methodology, B.B., I.D. and S.S.; software, B.B., S.S.; formal analysis, B.B., S.S.; writing—original draft preparation, B.B. and I.D.; writing—review and editing, B.B., I.D., S.S.; validation, B.B., I.D., S.S.; supervision, B.B. All authors have read and agreed to the published version of the manuscript.

Funding: This research received no external funding.

Data Availability Statement: Software codes are available at Zenodo: 10.5281/zenodo.17035818.

Acknowledgments: During the preparation of the manuscript, some figures were realized using https://www.biorender.com (accessed on 18 August 2025). The authors have reviewed and edited the output and take full responsibility for the content of this publication.

Conflicts of Interest: The authors declare no conflicts of interest.

References

1. Blanchini, F.; El-Samad, H.; Giordano, G.; Sontag, E.D. Control-theoretic methods for biological networks. In Proceedings of the 2018 IEEE Conference on Decision and Control (CDC), Miami, FL, USA, 17–19 December 2018; pp. 466–483.
2. Burlando, B. Loopomics: A new functional approach to life. *J. Appl. Physiol.* **2017**, *123*, 1011–1013. [CrossRef]
3. El-Samad, H. Biological feedback control-Respect the loops. *Cell Syst.* **2021**, *12*, 477–487. [CrossRef]
4. Munoz-Culla, M.; Irizar, H.; Gorostidi, A.; Alberro, A.; Osorio-Querejeta, I.; Ruiz-Martinez, J.; Olascoaga, J.; Lopez de Munain, A.; Otaegui, D. Progressive changes in non-coding RNA profile in leucocytes with age. *Aging* **2017**, *9*, 1202–1218. [CrossRef]
5. Saxton, R.A.; Sabatini, D.M. mTOR Signaling in Growth, Metabolism, and Disease. *Cell* **2017**, *168*, 960–976. [CrossRef]
6. Agorastos, A.; Chrousos, G.P. The neuroendocrinology of stress: The stress-related continuum of chronic disease development. *Mol. Psychiatry* **2022**, *27*, 502–513. [CrossRef]
7. Peper, J.S.; Brouwer, R.M.; van Leeuwen, M.; Schnack, H.G.; Boomsma, D.I.; Kahn, R.S.; Hulshoff Pol, H.E. HPG-axis hormones during puberty: A study on the association with hypothalamic and pituitary volumes. *Psychoneuroendocrinology* **2010**, *35*, 133–140. [CrossRef]
8. Mastorakos, G.; Pavlatou, M.G.; Mizamtsidi, M. The hypothalamic-pituitary-adrenal and the hypothalamic-pituitary-gonadal axes interplay. *Pediatr. Endocrinol. Rev.* **2006**, *3*, 172–181.
9. Caufriez, A.; Leproult, R.; Copinschi, G. Circadian profiles of progesterone, gonadotropins, cortisol and corticotropin in cycling and postmenopausal women. *Chronobiol. Int.* **2018**, *35*, 72–79. [CrossRef]
10. Rahman, S.A.; Grant, L.K.; Gooley, J.J.; Rajaratnam, S.M.W.; Czeisler, C.A.; Lockley, S.W. Endogenous Circadian Regulation of Female Reproductive Hormones. *J. Clin. Endocrinol. Metab.* **2019**, *104*, 6049–6059. [CrossRef]
11. Demori, I.; Losacco, S.; Giordano, G.; Mucci, V.; Blanchini, F.; Burlando, B. Fibromyalgia pathogenesis explained by a neuroendocrine multistable model. *PLoS ONE* **2024**, *19*, e0303573. [CrossRef]
12. Kottler, M.L.; Coussieu, C.; Valensi, P.; Levi, F.; Degrelle, H. Ultradian, circadian and seasonal variations of plasma progesterone and LH concentrations during the luteal phase. *Chronobiol. Int.* **1989**, *6*, 267–277. [CrossRef]
13. Elsner, C.W.; Buster, J.E.; Preston, D.L.; Killam, A.P. Interrelationships of circulating maternal steroid concentrations in third trimester pregnancies. III. Effect of intravenous cortisol infusion on maternal concentrations of estriol, 16 alpha-hydroxyprogesterone, 17 alpha-hydroxyprogesterone, progesterone, 20 alpha-dihydroprogesterone, delta 5-pregnenolone, delta5-pregnenolone sulfate, dehydroepiandrosterone sulfate, and cortisol. *J. Clin. Endocrinol. Metab.* **1979**, *49*, 30–33. [CrossRef]
14. Saketos, M.; Sharma, N.; Santoro, N.F. Suppression of the hypothalamic-pituitary-ovarian axis in normal women by glucocorticoids. *Biol. Reprod.* **1993**, *49*, 1270–1276. [CrossRef]
15. Segebladh, B.; Bannbers, E.; Moby, L.; Nyberg, S.; Bixo, M.; Backstrom, T.; Sundstrom Poromaa, I. Allopregnanolone serum concentrations and diurnal cortisol secretion in women with premenstrual dysphoric disorder. *Arch. Womens Ment. Health* **2013**, *16*, 131–137. [CrossRef]
16. Brownlee, K.K.; Moore, A.W.; Hackney, A.C. Relationship between circulating cortisol and testosterone: Influence of physical exercise. *J. Sports Sci. Med.* **2005**, *4*, 76–83.
17. Anderson, T.; Lane, A.R.; Hackney, A.C. Cortisol and testosterone dynamics following exhaustive endurance exercise. *Eur. J. Appl. Physiol.* **2016**, *116*, 1503–1509. [CrossRef]
18. Rubinow, D.R.; Roca, C.A.; Schmidt, P.J.; Danaceau, M.A.; Putnam, K.; Cizza, G.; Chrousos, G.; Nieman, L. Testosterone suppression of CRH-stimulated cortisol in men. *Neuropsychopharmacology* **2005**, *30*, 1906–1912. [CrossRef]
19. Oyola, M.G.; Handa, R.J. Hypothalamic-pituitary-adrenal and hypothalamic-pituitary-gonadal axes: Sex differences in regulation of stress responsivity. *Stress* **2017**, *20*, 476–494. [CrossRef]
20. Lehman, M.N.; Hileman, S.M.; Goodman, R.L. Neuroanatomy of the kisspeptin signaling system in mammals: Comparative and developmental aspects. *Adv. Exp. Med. Biol.* **2013**, *784*, 27–62. [CrossRef]
21. Goodman, R.L.; Lehman, M.N. Kisspeptin neurons from mice to men: Similarities and differences. *Endocrinology* **2012**, *153*, 5105–5118. [CrossRef]

22. Cravo, R.M.; Margatho, L.O.; Osborne-Lawrence, S.; Donato, J., Jr.; Atkin, S.; Bookout, A.L.; Rovinsky, S.; Frazao, R.; Lee, C.E.; Gautron, L.; et al. Characterization of Kiss1 neurons using transgenic mouse models. *Neuroscience* **2011**, *173*, 37–56. [CrossRef]
23. Miller, B.H.; Gore, A.C. N-Methyl-D-aspartate receptor subunit expression in GnRH neurons changes during reproductive senescence in the female rat. *Endocrinology* **2002**, *143*, 3568–3574. [CrossRef]
24. Ivanova, D.; O'Byrne, K.T. Optogenetics studies of kisspeptin neurons. *Peptides* **2023**, *162*, 170961. [CrossRef]
25. Ottem, E.N.; Godwin, J.G.; Krishnan, S.; Petersen, S.L. Dual-phenotype GABA/glutamate neurons in adult preoptic area: Sexual dimorphism and function. *J. Neurosci.* **2004**, *24*, 8097–8105. [CrossRef]
26. Putteeraj, M.; Soga, T.; Ubuka, T.; Parhar, I.S. A "Timed" Kiss Is Essential for Reproduction: Lessons from Mammalian Studies. *Front. Endocrinol.* **2016**, *7*, 121. [CrossRef]
27. Watanabe, M.; Fukuda, A.; Nabekura, J. The role of GABA in the regulation of GnRH neurons. *Front. Neurosci.* **2014**, *8*, 387. [CrossRef]
28. Maffucci, J.A.; Gore, A.C. Chapter 2: Hypothalamic neural systems controlling the female reproductive life cycle gonadotropin-releasing hormone, glutamate, and GABA. *Int. Rev. Cell Mol. Biol.* **2009**, *274*, 69–127. [CrossRef]
29. Di Giorgio, N.P.; Bizzozzero-Hiriart, M.; Libertun, C.; Lux-Lantos, V. Unraveling the connection between GABA and kisspeptin in the control of reproduction. *Reproduction* **2019**, *157*, R225–R233. [CrossRef]
30. Li, X.F.; Bowe, J.E.; Kinsey-Jones, J.S.; Brain, S.D.; Lightman, S.L.; O'Byrne, K.T. Differential role of corticotrophin-releasing factor receptor types 1 and 2 in stress-induced suppression of pulsatile luteinising hormone secretion in the female rat. *J. Neuroendocr.* **2006**, *18*, 602–610. [CrossRef]
31. Breen, K.M.; Karsch, F.J. New insights regarding glucocorticoids, stress and gonadotropin suppression. *Front. Neuroendocr.* **2006**, *27*, 233–245. [CrossRef]
32. Phumsatitpong, C.; Wagenmaker, E.R.; Moenter, S.M. Neuroendocrine interactions of the stress and reproductive axes. *Front. Neuroendocr.* **2021**, *63*, 100928. [CrossRef]
33. Herman, J.P.; Mueller, N.K.; Figueiredo, H. Role of GABA and glutamate circuitry in hypothalamo-pituitary-adrenocortical stress integration. *Ann. N. Y. Acad. Sci.* **2004**, *1018*, 35–45. [CrossRef]
34. Rasiah, N.P.; Loewen, S.P.; Bains, J.S. Windows into stress: A glimpse at emerging roles for CRH(PVN) neurons. *Physiol. Rev.* **2023**, *103*, 1667–1691. [CrossRef]
35. Maguire, J. The relationship between GABA and stress: 'It's complicated'. *J. Physiol.* **2018**, *596*, 1781–1782. [CrossRef]
36. Levy, B.H.; Tasker, J.G. Synaptic regulation of the hypothalamic-pituitary-adrenal axis and its modulation by glucocorticoids and stress. *Front. Cell Neurosci.* **2012**, *6*, 24. [CrossRef]
37. Aguilera, G.; Liu, Y. The molecular physiology of CRH neurons. *Front. Neuroendocr.* **2012**, *33*, 67–84. [CrossRef]
38. Gunn, B.G.; Cunningham, L.; Mitchell, S.G.; Swinny, J.D.; Lambert, J.J.; Belelli, D. GABAA receptor-acting neurosteroids: A role in the development and regulation of the stress response. *Front. Neuroendocr.* **2015**, *36*, 28–48. [CrossRef]
39. Marraudino, M.; Miceli, D.; Farinetti, A.; Ponti, G.; Panzica, G.; Gotti, S. Kisspeptin innervation of the hypothalamic paraventricular nucleus: Sexual dimorphism and effect of estrous cycle in female mice. *J. Anat.* **2017**, *230*, 775–786. [CrossRef]
40. Rao, Y.S.; Mott, N.N.; Pak, T.R. Effects of kisspeptin on parameters of the HPA axis. *Endocrine* **2011**, *39*, 220–228. [CrossRef]
41. Angelopoulou, E.; Quignon, C.; Kriegsfeld, L.J.; Simonneaux, V. Functional Implications of RFRP-3 in the Central Control of Daily and Seasonal Rhythms in Reproduction. *Front. Endocrinol.* **2019**, *10*, 183. [CrossRef]
42. Ullah, R.; Batool, A.; Wazir, M.; Naz, R.; Rahman, T.U.; Wahab, F.; Shahab, M.; Fu, J. Gonadotropin inhibitory hormone and RF9 stimulate hypothalamic-pituitary-adrenal axis in adult male rhesus monkeys. *Neuropeptides* **2017**, *66*, 1–7. [CrossRef]
43. Iwasa, T.; Matsuzaki, T.; Yano, K.; Irahara, M. Gonadotropin-Inhibitory Hormone Plays Roles in Stress-Induced Reproductive Dysfunction. *Front. Endocrinol.* **2017**, *8*, 62. [CrossRef]
44. Molnar, C.S.; Kallo, I.; Liposits, Z.; Hrabovszky, E. Estradiol down-regulates RF-amide-related peptide (RFRP) expression in the mouse hypothalamus. *Endocrinology* **2011**, *152*, 1684–1690. [CrossRef]
45. Poling, M.C.; Kim, J.; Dhamija, S.; Kauffman, A.S. Development, sex steroid regulation, and phenotypic characterization of RFamide-related peptide (Rfrp) gene expression and RFamide receptors in the mouse hypothalamus. *Endocrinology* **2012**, *153*, 1827–1840. [CrossRef]
46. Angelopoulou, E.; Inquimbert, P.; Klosen, P.; Anderson, G.; Kalsbeek, A.; Simonneaux, V. Daily and Estral Regulation of RFRP-3 Neurons in the Female Mice. *J. Circadian Rhythm.* **2021**, *19*, 4. [CrossRef]
47. Ronnekleiv, O.K.; Qiu, J.; Kelly, M.J. Hypothalamic Kisspeptin Neurons and the Control of Homeostasis. *Endocrinology* **2022**, *163*, bqab253. [CrossRef]
48. Blanchini, F.; Cuba Samaniego, C.; Franco, E.; Giordano, G. Aggregates of Monotonic Step Response Systems: A Structural Classification. *IEEE Trans. Control. Netw. Syst.* **2018**, *5*, 782–792.

49. Jones, J.R.; Chaturvedi, S.; Granados-Fuentes, D.; Herzog, E.D. Circadian neurons in the paraventricular nucleus entrain and sustain daily rhythms in glucocorticoids. *Nat. Commun.* **2021**, *12*, 5763. [CrossRef]
50. Skinner, D.C.; Evans, N.P.; Delaleu, B.; Goodman, R.L.; Bouchard, P.; Caraty, A. The negative feedback actions of progesterone on gonadotropin-releasing hormone secretion are transduced by the classical progesterone receptor. *Proc. Natl. Acad. Sci. USA* **1998**, *95*, 10978–10983. [CrossRef]
51. Alon, U. *An Introduction to Systems Biology: Design Principles of Biological Circuits*; Chapman and Hall/CRC: Boca Raton, FL, USA, 2019; p. 320.
52. Demori, I.; Giordano, G.; Mucci, V.; Losacco, S.; Marinelli, L.; Massobrio, P.; Blanchini, F.; Burlando, B. Thalamocortical bistable switch as a theoretical model of fibromyalgia pathogenesis inferred from a literature survey. *J. Comput. Neurosci.* **2022**, *50*, 471–484. [CrossRef]
53. Klipp, E.; Liebermeister, W.; Wierling, C.; Kowald, A. *Systems Biology: A Textbook*; Wiley-Blackwell: Hoboken, NJ, USA, 2016; p. 504.
54. Ferrell, J.E., Jr. Self-perpetuating states in signal transduction: Positive feedback, double-negative feedback and bistability. *Curr. Opin. Cell Biol.* **2002**, *14*, 140–148. [CrossRef]
55. Bintu, L.; Buchler, N.E.; Garcia, H.G.; Gerland, U.; Hwa, T.; Kondev, J.; Phillips, R. Transcriptional regulation by the numbers: Models. *Curr. Opin. Genet. Dev.* **2005**, *15*, 116–124. [CrossRef]
56. Russell, G.; Lightman, S. The human stress response. *Nat. Rev. Endocrinol.* **2019**, *15*, 525–534. [CrossRef]
57. Mucci, V.; Demori, I.; Browne, C.J.; Deblieck, C.; Burlando, B. Fibromyalgia in Pregnancy: Neuro-Endocrine Fluctuations Provide Insight into Pathophysiology and Neuromodulation Treatment. *Biomedicines* **2023**, *11*, 615. [CrossRef]
58. Burlando, B. A general hypothesis of multistable systems in pathophysiology. *F1000Res* **2022**, *11*, 906. [CrossRef]
59. Desroches, M.; Guckenheimer, J.; Krauskopf, B.; Kuehn, C.; Osinga, H.M.; Wechselberger, M. Mixed-Mode Oscillations with Multiple Time Scales. *SIAM Rev.* **2012**, *54*, 211–288.
60. Koseska, A.; Volkov, E.; Kurths, J. Oscillation quenching mechanisms: Amplitude vs. oscillation death. *Phys. Rep.* **2013**, *531*, 173–199. [CrossRef]
61. Tolin, D.F.; Foa, E.B. Sex differences in trauma and posttraumatic stress disorder: A quantitative review of 25 years of research. *Psychol. Bull.* **2006**, *132*, 959–992. [CrossRef]
62. Albert, P.R. Why is depression more prevalent in women? *J. Psychiatry Neurosci.* **2015**, *40*, 219–221. [CrossRef]
63. de Kloet, E.R.; Joels, M.; Holsboer, F. Stress and the brain: From adaptation to disease. *Nat. Rev. Neurosci.* **2005**, *6*, 463–475. [CrossRef]
64. Anacker, C.; Zunszain, P.A.; Carvalho, L.A.; Pariante, C.M. The glucocorticoid receptor: Pivot of depression and of antidepressant treatment? *Psychoneuroendocrinology* **2011**, *36*, 415–425. [CrossRef]
65. Gjerstad, J.K.; Lightman, S.L.; Spiga, F. Role of glucocorticoid negative feedback in the regulation of HPA axis pulsatility. *Stress* **2018**, *21*, 403–416. [CrossRef]
66. Turner, B.B. Sex difference in glucocorticoid binding in rat pituitary is estrogen dependent. *Life Sci.* **1990**, *46*, 1399–1406. [CrossRef]
67. Agba, O.B.; Lausser, L.; Huse, K.; Bergmeier, C.; Jahn, N.; Groth, M.; Bens, M.; Sahm, A.; Gall, M.; Witte, O.W.; et al. Tissue-, sex-, and age-specific DNA methylation of rat glucocorticoid receptor gene promoter and insulin-like growth factor 2 imprinting control region. *Physiol. Genom.* **2017**, *49*, 690–702. [CrossRef]
68. Vandevyver, S.; Dejager, L.; Libert, C. On the trail of the glucocorticoid receptor: Into the nucleus and back. *Traffic* **2012**, *13*, 364–374. [CrossRef]
69. Arango-Lievano, M.; Lambert, W.M.; Bath, K.G.; Garabedian, M.J.; Chao, M.V.; Jeanneteau, F. Neurotrophic-priming of glucocorticoid receptor signaling is essential for neuronal plasticity to stress and antidepressant treatment. *Proc. Natl. Acad. Sci. USA* **2015**, *112*, 15737–15742. [CrossRef]
70. Van Moortel, L.; Gevaert, K.; De Bosscher, K. Improved Glucocorticoid Receptor Ligands: Fantastic Beasts, but How to Find Them? *Front. Endocrinol.* **2020**, *11*, 559673. [CrossRef]
71. Meltzer-Brody, S.; Colquhoun, H.; Riesenberg, R.; Epperson, C.N.; Deligiannidis, K.M.; Rubinow, D.R.; Li, H.; Sankoh, A.J.; Clemson, C.; Schacterle, A.; et al. Brexanolone injection in post-partum depression: Two multicentre, double-blind, randomised, placebo-controlled, phase 3 trials. *Lancet* **2018**, *392*, 1058–1070. [CrossRef]
72. Deligiannidis, K.M.; Meltzer-Brody, S.; Maximos, B.; Peeper, E.Q.; Freeman, M.; Lasser, R.; Bullock, A.; Kotecha, M.; Li, S.; Forrestal, F.; et al. Zuranolone for the Treatment of Postpartum Depression. *Am. J. Psychiatry* **2023**, *180*, 668–675. [CrossRef]
73. Caparros-Gonzalez, R.A.; Romero-Gonzalez, B.; Strivens-Vilchez, H.; Gonzalez-Perez, R.; Martinez-Augustin, O.; Peralta-Ramirez, M.I. Hair cortisol levels, psychological stress and psychopathological symptoms as predictors of postpartum depression. *PLoS ONE* **2017**, *12*, e0182817. [CrossRef]

74. Iliadis, S.I.; Comasco, E.; Sylven, S.; Hellgren, C.; Sundstrom Poromaa, I.; Skalkidou, A. Prenatal and Postpartum Evening Salivary Cortisol Levels in Association with Peripartum Depressive Symptoms. *PLoS ONE* **2015**, *10*, e0135471. [CrossRef]
75. Burlando, B.; Demori, I. Neurosteroids as a possible new horizon in the treatment of fibromyalgia. *Med. Hypotheses* **2024**, *191*, 111444.